Alternations of Brain Structural Connectivity after Unilateral Upper-limb Amputation

Xiaoli Guo[1], Ruihao Liu[1], Jincheng Lu[1], Chaowei Wu[1], Yuanyuan Lyu[1], Zhuo Wang[1], Jianbo Xiang[2], Changjie Pan[2], Shanbao Tong[1,*]

[1]School of Biomedical Engineering, Shanghai Jiao Tong University, Shanghai 200240, China.

[2]Department of Radiology, the 2nd 10 People's Hospital of Changzhou Affiliated to Nanjing Medical University, Changzhou, Jiangsu 213000, China

*Corresponding authors: Shanbao Tong, School of biomedical engineering, Shanghai Jiao Tong University, 800 Dongchuan Road, Shanghai 200240, China. Tel.: +862134205138, e-mail: stong@sjtu.edu.cn.

Abstract

Previous studies have indicated that amputation induces reorganization of functional brain network. However, the influence of amputation on structural brain network remains unexplored. In this study, using diffusion tensor imaging (DTI), we aimed to investigate the alternations of fractional anisotropy (FA) network after unilateral upper-limb amputation. The FA network of the dominant-side amputees showed reduced mean strength, density and increased characteristic path length compared with that of healthy controls; while the nondominant-side amputees showed comparable global metrics of FA network as healthy controls. The nodal strength in the contralateral sensorimotor system and visual areas was reduced in both dominant- and nondominant-side amputees. In particular, the strength of the contralateral postcentral gyrus was significantly negatively correlated with residual limb usage in the dominant-side amputees, representing a use-dependent reorganization. In addition, the strength of the contralateral middle temporal gyrus was significantly positively correlated with the magnitude of phantom limb sensation. Our results suggested degeneration of FA network after unilateral upper-limb amputation, which was especially prominent in the dominant-side amputees.

Key words: unilateral upper-limb amputation, diffusion tensor imaging, fractional anisotropy, structural brain network

Introduction

Limb amputation not only impacts the peripheral nervous system, but also induces reorganization of the brain, mostly due to the lack of sensory input from and overt motor output to the missing limb. Neuroimaging studies have shown that limb amputation induces morphometric changes as well as functional remapping in gray matter (GM), prominently in the primary sensory (S1) and motor (M1) cortices [1]. In addition, cortical reorganization after limb amputation has also been observed at a network-level scale. Using resting-state functional magnetic resonance imaging (fMRI), Pawela *et al.* reported a substantial disruption of interhemispheric sensorimotor cortical connectivity in animals after limb deafferentation [2], and Makin *et al.* found reduced inter-regional functional connectivities in the primary sensorimotor cortex in amputees [3, 4]. Using electroencephalography (EEG), Lyu *et al*. found that the alpha network of upper-limb amputees presented increased clustering coefficient, decreased characteristic path length and increased small-worldness compared with that of healthy controls [5].

Brain reorganization following limb amputation is not restricted to the GM but also happens in the white matter (WM). Using diffusion tensor imaging (DTI), reduction in fractional anisotropy (FA) values in the corpus callosum (CC) [6], unaffected superior corona radiate, WM regions underlying the unaffected temporal lobe and affected premotor cortex [7], and increased in axial diffusivity (AD), radial diffusivity (RD) and mean diffusivity (MD) values in region II of the CC [8], have been found in lower-limb amputees. However, the change of WM after upper-limb amputation has been not yet explored.

In addition to WM microstructures, graph theoretical analysis provides a framework for

understanding the topological organization of the WM structural networks [9]. The WM networks, which are considered as structural substrates of functional networks, also exhibit small-worldness and modularity [10]. We hypothesized that amputation might also disrupt the structural network topology. However, to our knowledge, no studies have reported the topological changes in the WM structural networks after amputation. In the present study, using DTI tractography and graph theoretical approaches, we aimed to explore the topological changes in the WM networks after upper-limb amputation. Considering the influence of white matter asymmetry between two hemispheres [11] and the possibility for different brain reorganization involved in amputees who lost their dominant or nondominant hand [12], right- and left-side upper-limb amputees were compared with healthy controls, respectively.

Materials and Methods

Participants

Sixteen right-side upper-limb amputees (age: 53.44 ± 8.09 years; sex: 11M/5F; time since amputation: 25.81 ± 11.35 years), seven left-side upper-limb amputees (age: 50.57 ± 7.76 years; sex: 6M/1F; time since amputation: 18.00 ± 16.94 years), and fifteen healthy controls (age: 51.20 ± 9.43 years; sex: 11M/4F) participated in this study. Independent t-tests showed that either right-side or left-side amputees did not differ significantly with controls in age (both $p > 0.483$). All participants except one amputee (A19) were right-handed according to a Chinese version of a standardized handedness inventory [13]. A19 could not complete the inventory because he received an amputation at the age of two. All participants reported no history of neurological or mental disorders. Each subject signed written informed consent before the experiment and received financial compensation after the experiment. The protocols of this

study were in compliance with the Declaration of Helsinki.

Phantom limb pain and non-painful phantom limb sensation were assessed by a standardized interview [14] and a modified version of the West Haven-Yale Multidimensional Pain Inventory [15]. If amputees reported pain/sensation experience within the past three months, they were required to localize the pain/sensation, and describe the quality of the pain/sensation. Then each amputee reported a score on a 0-10 scale based on the average intensity of his/her pain/sensation within the last month (0 = no pain/no sensation; 10 = worst pain imaginable/most intense sensation). The use of the residual arm in daily activities was assessed using a questionnaire designed and validated by Makin, Scholz [4], which focuses on the frequency with which participants incorporate their residual arm (either directly or by using a prosthesis) in daily activities. The questionnaire includes 27 items in total, covering a comprehensive range of commonly encountered actions, such as holding up a phone or carrying bags. Each item was scored according to the frequency of residual limb usage (0: never; 1: sometimes; 2: very often). The sum of all items, ranging from 0 to 54, was used as the score of residual limb usage. Four amputees (1M/3F, amputation side: 3R/1L, amputation level: all below elbow) wore cosmetic prostheses in their everyday life (only when awake). The detailed demographic and amputation-related information of the amputees is summarized in Table 1.

Table 1 Demographic and amputation-related information of amputees.

ID	Sex	Age (yrs)	Amputation			Residual limb Usage	Prosthesis	PLP	PLS
			Side and level	Cause	Time (yrs)				
A1	M	59	R, below shoulder	Accident	32	0	N	8	6
A2	M	71	R, below shoulder	Accident	39	2	N	0	5
A3	M	55	R, below elbow	Accident	16	8	N	0	9
A4	M	57	R, below elbow	Accident	20	13	N	0	7

A5	M	40	R, below shoulder	Accident	21	4	N	0	3
A6	F	46	R, below shoulder	Accident	17	6	N	0	7
A7	M	56	R, below wrist	Accident	32	12	N	0	6
A8	M	45	R, below elbow	Accident	28	12	N	0	0
A9	M	58	R, below wrist	Accident	18	17	N	0	6
A10	M	55	R, below shoulder	Accident	40	10	N	0	0
A11	M	59	R, below shoulder	Accident	44	1	N	0	0
A12	M	47	R, below shoulder	Accident	30	1	N	8	5
A13	F	46	R, below elbow	Accident	12	7	Y	0	5
A14	F	63	R, below elbow	Accident	41	13	Y	0	3
A15	F	53	R, below shoulder	Accident	13	2	N	0	0
A16	F	45	R, below wrist	Accident	10	5	Y	0	0
A17	M	42	L, below wrist	Accident	5	14	N	0	0
A18	M	47	L, below elbow	Accident	2	9	Y	0	4
A19	M	44	L, below elbow	Accident	42	13	N	0	0
A20	M	61	L, below elbow	Accident	8	4	N	0	0
A21	M	61	L, below elbow	Accident	34	17	N	0	10
A22	F	47	L, below wrist	Accident	31	53	N	0	9
A23	M	52	L, below shoulder	Accident	4	0	N	7	6

M = Male, F = Female; yrs = years; L = left, R = right; prosthesis = whether or not wearing any prosthesis; Y = yes, N = no; PLP = phantom limb pain, PLS = phantom limb sensation.

PLP and RLP were reported on a 0-10 scale based on the average intensity of his/her pain/sensation within the last month (0 = no pain/no sensation, 10 = worst pain imaginable/most intense sensation).

MRI Acquisition

All MRI brain scans were acquired at the Second People's Hospital of Changzhou on a 3T system (Philips, Achieva 3.0T TX, Netherlands) with an 8-channel head coil. Whole brain anatomical T1-weighted images were obtained in a sagittal direction with a 3D-TFE sequence (TR = 8.2 ms, TE =3.7 ms, flip angle = 8°, FOV = 250 × 250 mm2, number of slices = 162, imaging matrix = 256 × 256, voxel size = 0.976 × 0.976 × 1.00 mm3). Diffusion tensor images (DTI) were acquired using a spinecho echo-planar imaging sequence (TR = 7444.428 ms, TE

= 85 ms, flip angle = 90°, NSA = 2, FOV = 224 × 224 mm2, number of slices = 60, slice thickness = 2 mm, no gap, matrix = 112 × 112)

orientation = axial; 32 nonlinear diffusion weighting gradient directions

with b = 800 s/mm2 and 1 additional image without diffusion weighting [i.e., b = 0 s/mm2]).

DTI Data Pre-Processing and Network Definition

DTI data preprocessing was performed using a matlab toolbox "Pipeline for Analyzing braiN Diffusion imAges (PANDA)" [16]. First, the DTI images were corrected for head motion and eddy current distortions using the FMRIB's Diffusion Toolbox (FDT, version 5.0; http://www.fmrib.ox.ac.uk/fsl) [17]. Then, the skull and non-brain tissue were remove from images using the FSL Brain Extraction Tool (BET) [18]. Next, the fractional anisotropy (FA), a marker of fiber tract integrity, was calculated for each voxel using the DTIFIT tool [19].

The brain network includes 90 nodes, which were defined using the Automated Anatomical Labeling (AAL) atlas [20]. Briefly, individual T1-weighted images were coregistered to the b0 images in the DTI space using an affine transformation. The transformed T1 images were nonlinearly registered to the MNI-ICBM152_2mm template. Using the inverse transformations, the AAL atlas was warped from the MNI space to the DTI native space. DTI tractography was carried out using a deterministic tractographic method based on fiber assignment by continuous tracking (FACT) algorithm [21], which was terminated when it turned an angle greater than 45° or reached a voxel with an FA less than 0.15. In order to reduce the risk of false-positive connections, two nodes were considered structurally connected only when at least 3 fibers were reconstructed between them [22, 23]. FA weighted network was constructed, in which the weight of the edges was defined as the mean FA value of the

connected fibers between each two nodes.

Graph Analysis

(1) Global and Nodal Strength

For a weighted undirected network *G* with *N* nodes and *E* edges, the mean strength of *G* is calculated as the average of the strengths across all the nodes in the network:

$$S(G) = \frac{1}{N}\sum_{j=1}^{N} S_j.$$

Here, S_j is the strength of node j, which is calculated as the sum of the edge weights linking to the node j.

(2) Density

The density of a network is defined as the ratio of the number of real edges to the number of total possible edges:

$$D(G) = \frac{2E}{N(N-1)}.$$

(3) Global Clustering Coefficient

The clustering coefficient of a network is defined as the mean of clustering coefficients across all the nodes:

$$C(G) = \frac{1}{N}\sum_{j=1}^{N} C_j.$$

C_j is the clustering coefficient of node j. In a weighted undirected network, it is calculated as:

$$C_j = \frac{1}{S_j(k_j-1)}\sum_{(i,k)} \frac{w_{ij}+w_{jk}}{2} a_{ij}a_{ik}a_{jk}.$$

Here, S_j is the strength of the node j, k_j is the degree of node j, w_{ij} is the edge weight between nodes i and j, and $a_{ij} = 1$, if $w_{ij} > 0$, otherwise $a_{ij} = 0$.

(4) Characteristic path length

The characteristic path length of a network is defined as:

$$L = \frac{N(N-1)}{\sum_{i=1}^{N}\sum_{j\neq i}^{N} 1/l_{ij}},$$

where l_{ij} is the shortest path length between nodes i and j. The length of an edge is obtained by computing the reciprocal of the edge weight w_{ij}.

Statistical Analysis

In order to identify changes in FA network after unilateral upper-limb amputation, independent two-tailed t-tests were employed to compare global strength, density, clustering coefficient, characteristic path length, and nodal strength between amputees and controls. Left-side or right-side amputees were compared with controls respectively to exclude influence of white matter asymmetry [24]. Rough false discovery rate (rFDR) correction was used for multiple comparisons in the statistical analysis of nodal strength ($p < 0.025$) [25].

Then, we tested whether the observed changes in FA network in amputees are related to amputation-related variables using Pearson's correlation. In particular, we were interested in identifying the potential roles of time since amputation, residual limb usage, PLP and PLS. To exclude the potential influence of age, the observed significant correlations were further verified using partial correlation analyses (adjusted for age).

Results

Global Metrics

Overall, the connectivity pattern of FA network was similar in healthy controls and amputees (Fig. 1A). However, the FA network of the right-side amputees was significantly reduced in mean strength (right-side amputees = 2.429 ± 0.164, controls = 2.628 ± 0.159, p =

0.002, Fig. 1B), either in the right (p = 0.023, Fig. 1C) or left (p = 0.005, Fig. 1D) hemisphere, suggesting a global impairment of the FA network after right-side upper-limb amputation. The mean strength in the left hemisphere was higher than that in the right hemisphere in healthy control (left: 2.696 ± 0.219, right: 2.555 ± 0.205, p = 0.003), while the mean strength was comparable in two hemispheres in the right-side amputees (left: 2.461 ± 0.216, right: 2.396 ± 0.163, p = 0.205). The density of the FA network was also significantly decreased in the right-side amputees (right-side amputees = 0.071 ± 0.004, controls = 0.075 ± 0.004, p = 0.003, Fig. 1E). The clustering coefficient of the FA network of the right-side amputees was comparable to healthy controls (right-side amputees = 0.481 ± 0.020, controls = 0.476 ± 0.019, p = 0.493, Fig.1F), while the characteristic path length was significantly increased in the right-side amputees (right-side amputees = 2.835 ± 0.102, controls = 2.732 ± 0.095, p = 0.007, Fig.1G). However, these global parameters of FA network did not show significant correlations with amputation-related variables in the right-side amputees (all p > 0.22).

No significant differences in global parameters of FA network were observed when comparing between the left-side amputees and healthy controls (all p > 0.19, Fig.1).

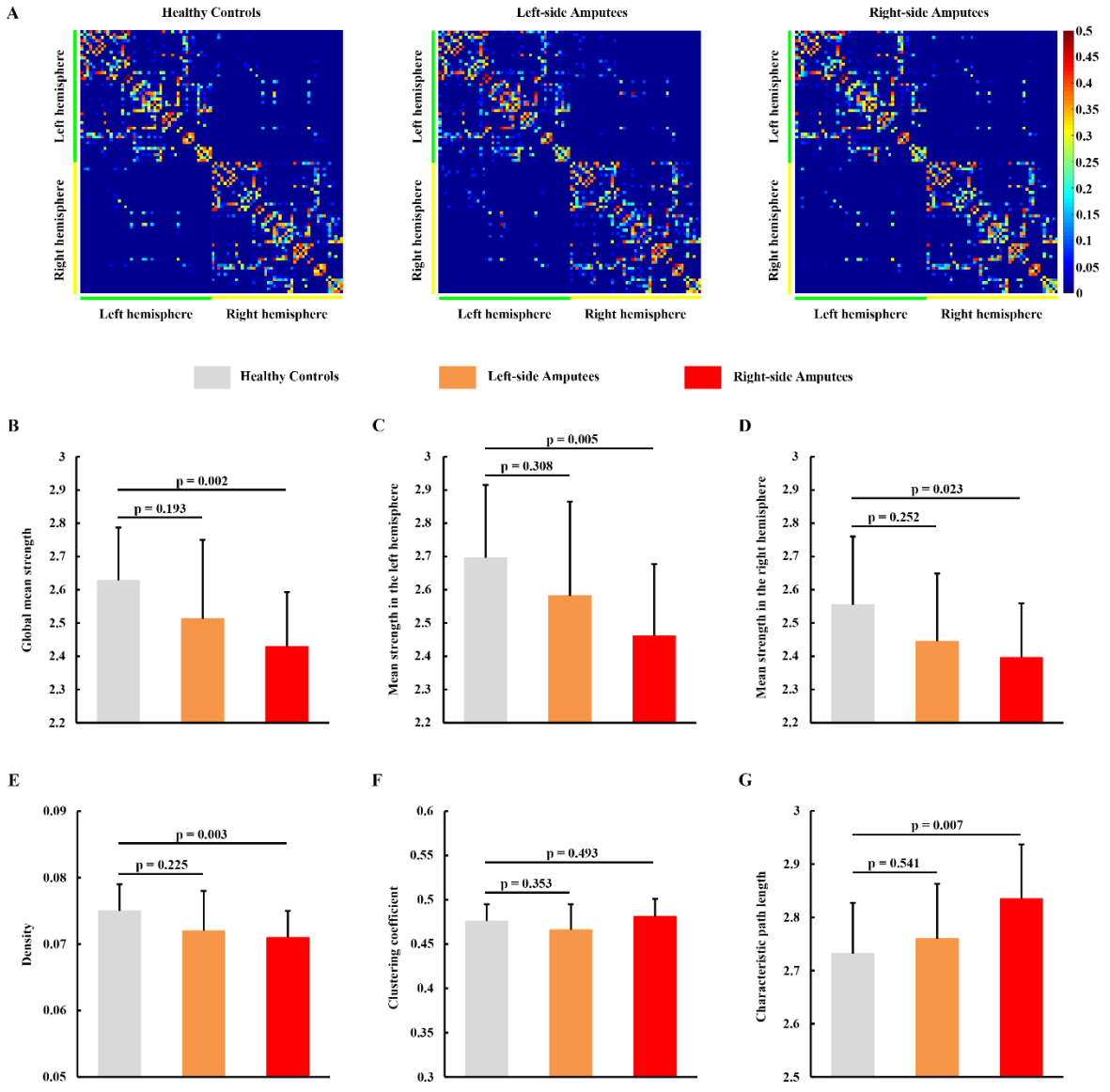

Figure 1. Comparison of global metrics of FA network among right-side amputees, left-side amputees and healthy controls. (A) The mean matrices; (B) global mean strength; (C) mean strength in the left hemisphere; (D) mean strength in the right hemisphere; (E) density; (F) clustering coefficient; (G) characteristic path length. Error bars indicate the standard deviation from the mean.

Nodal Strength

The nodal strength was asymmetric between two hemispheres in healthy controls. The

nodal strength was significantly larger in the left middle frontal gyrus, olfactory cortex, medial superior frontal gyrus, lingual gyrus, middle occipital gyrus and inferior temporal gyrus compared with the right counterparts; while the nodal strength was significantly larger in the right angular gyrus, temporal pole/ middle temporal gyrus, calcarine fissure and surrounding cortex compared with the left counterparts (all $p < 0.025$, see Fig. 2A and Table 2).

Table2. Brain regions showing significantly different nodal strength between two hemispheres in healthy controls.

Region	Nodal Strength		t value	p value
	Right	Left		
Brain regions with larger nodal strength in the left hemisphere				
Middle frontal gyrus	1.86 ± 0.46	2.64 ± 0.69	-3.301	0.005
Olfactory cortex	1.65 ± 0.40	2.40 ± 0.64	-4.023	0.001
Medial superior frontal gyrus	1.61 ± 0.66	2.09 ± 0.76	-2.604	0.021
Lingual gyrus	2.53 ± 0.65	3.34 ± 0.74	-3.308	0.005
Middle occipital gyrus	2.66 ± 0.93	4.38 ± 0.88	-7.222	<0.001
Inferior temporal gyrus	2.03 ± 0.35	2.35 ± 0.44	-3.467	0.004
Brain regions with larger nodal strength in the right hemisphere				
Angular gyrus	2.87 ± 0.71	1.22 ± 0.54	5.907	<0.001
Temporal pole/ middle temporal gyrus	1.63 ± 0.37	1.24 ± 0.38	3.164	0.007
Calcarine fissure and surrounding cortex	4.96 ± 1.69	4.01 ± 1.21	2.771	0.015

The right-side amputees presented a reduced strength in widely distributed brain regions, including the postcentral gyrus, paracentral lobule, temporal pole/middle temporal gyrus, middle and inferior temporal gyrus and inferior occipital gyrus in the left hemisphere which is contralateral to the amputation side, and the right (ipsilateral) calcarine fissure and surrounding cortex, supramarginal gyrus and inferior temporal gyrus (all $p < 0.025$, see Fig. 2B and Table 3). The left-side amputees presented a reduced nodal strength in the right (contralateral) precentral gyrus, medial superior frontal gyrus, temporal pole/middle temporal gyrus, inferior occipital gyrus, and the left (ipsilateral) paracentral lobule and parahippocampal gyrus, and showed an increased nodal strength in the left (ipsilateral) superior parietal gyrus (all $p < 0.025$,

see Fig. 2C and Table 4).

Table 3. Brain regions showing reduced nodal strength in the right-side amputees.

Region	Nodal Strength		t value	p value
	Amputees	Controls		
Left postcentral gyrus	2.79 ± 0.57	3.50 ± 0.65	-2.657	0.013
Left inferior occipital gyrus	1.23 ± 0.28	1.77 ± 0.61	-3.120	0.006
Left paracentral lobule	1.23 ± 0.45	1.71 ± 0.24	-2.426	0.022
Left temporal pole/middle temporal gyrus	0.89 ± 0.42	1.63 ± 0.37	-2.451	0.021
Left middle temporal gyrus	2.42 ± 0.48	2.93 ± 0.48	-2.946	0.006
Left inferior temporal gyrus	1.74 ± 0.53	2.35 ± 0.44	-3.527	0.001
Right calcarine fissure and surrounding cortex	3.71 ± 0.80	4.96 ± 1.69	-2.608	0.017
Right supramarginal gyrus	2.06 ± 0.76	2.56 ± 0.94	-3.049	0.005
Right inferior temporal gyrus	1.67 ± 0.45	2.35 ± 0.44	-2.429	0.022

Table 4. Brain regions showing different nodal strength between the left-side amputees and controls.

Region	Nodal Strength		t value	p value
	Amputees	Controls		
Brain regions with reduced nodal strength in the left-side amputees				
Right precental gyrus	3.80 ± 0.64	4.50 ± 0.74	-2.461	0.024
Right medial superior frontal gyrus	0.94 ± 0.40	1.61 ± 0.66	-2.476	0.022
Right temporal pole/middle temporal gyrus	1.18 ± 0.17	1.63 ± 0.37	-3.003	0.007
Right inferior occipital gyrus	1.02 ± 0.58	1.56 ± 0.45	-2.425	0.025
Left paracentral lobule	1.05 ± 0.34	1.57 ± 0.34	-3.384	0.003
Left parahippocampal gyrus	1.50 ± 0.38	2.25 ± 0.93	-2.671	0.015
Brain regions with increased nodal strength in the left-side amputees				
Left superior parietal gyrus	2.09 ± 0.49	1.56 ± 0.41	-2.644	0.016

In the right-side amputees, the strength of the contralateral postcentral gyrus was significantly negatively correlated with residual limb usage (Pearson's correlation, $r = -0.610$, $p = 0.012$, Fig. 3A). The strength of the contralateral middle temporal gyrus was significantly positively correlated with the PLS magnitude (Pearson's correlation, $r = 0.703$, $p = 0.002$, Fig. 3B). Partial correlation analyses (controlled for age) suggested that these correlations were not

affected by age (r = -0.647, p = 0.009; r = 0.762, p = 0.001, respectively). In the left-side amputees, we did not find any significant correlation between FA network parameters and amputation-related variables.

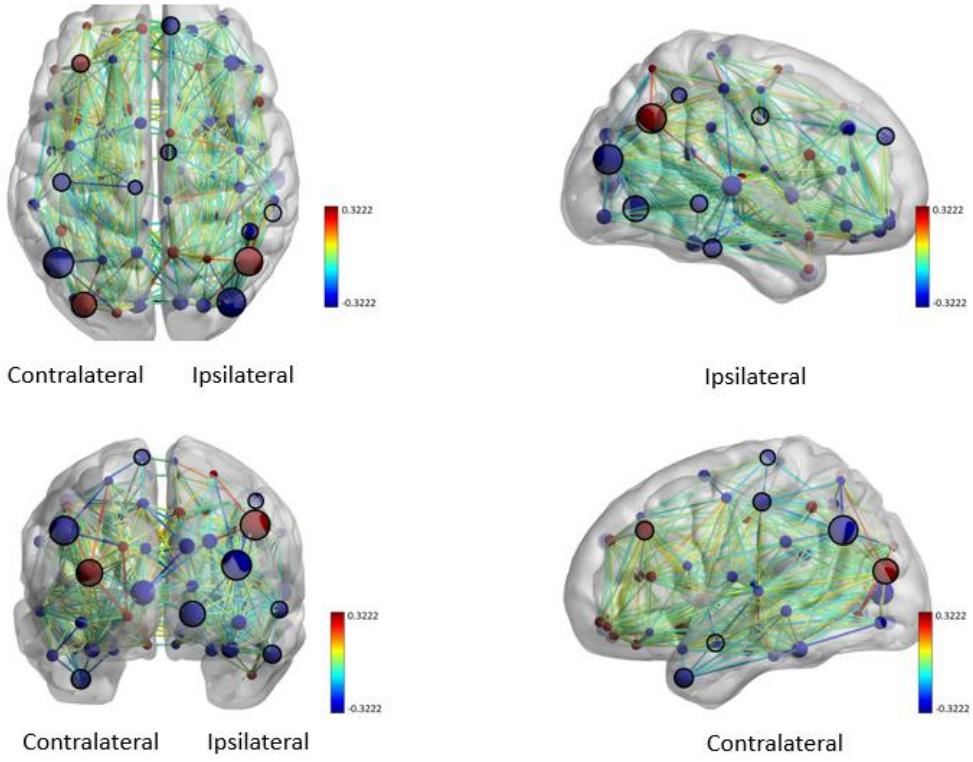

Figure 2. (A) Differences in nodal strength between brain regions in two hemispheres in healthy controls. (B) Differences in nodal strength between right-side amputees and healthy controls. (C) Differences in nodal strength between left-side amputees and healthy controls.

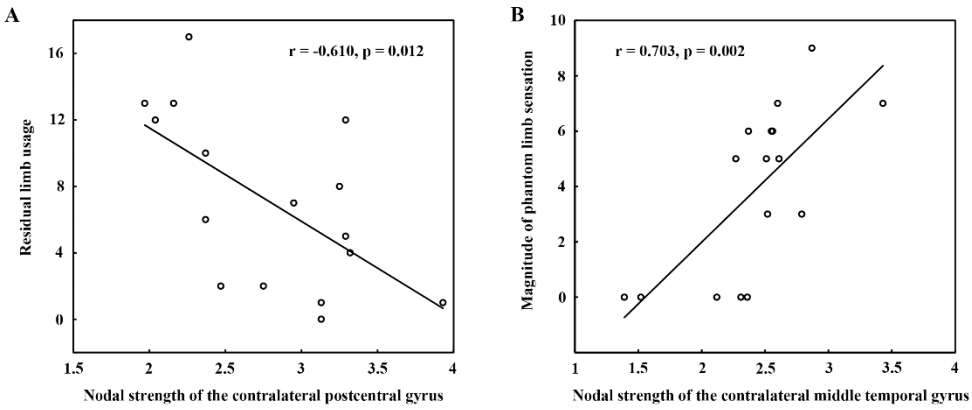

Figure 3 Correlations between the nodal strength and amputation-related variables in the right-side amputees. (A) Plots showing the significant negative correlation between the strength of the left (contralateral) postcentral gyrus and residual limb usage. (B) Plots showing the significant positive correlation between the strength of the left (contralateral) middle temporal gyrus and the magnitude of phantom limb sensation.

Discussion

The FA network was degraded after right-side upper-limb amputation. The right-side amputees presented a global reduction in the strength and density of the FA network. FA which reflects myelination degree, axonal density and/or integrity [26, 27], is often used as an indicator of WM integrity [28]. Therefore, our results suggested a typical amputation-related neurodegenerative phenomenon with a disruption of WM integrity in the whole brain. Both the global and nodal strength suggested that the degeneration of FA network was significant either in the contralateral or ipsilateral hemisphere, which might due to the reduced interhemispheric connectivity after amputation [6, 8]. The characteristic path length, which reflects the global integration of brain networks [29], was significantly increased in the right-side amputees, suggesting that large-scale interactions of spatially segregated modules was affected by dominant-side upper-limb amputation. The alternations of FA network seemed only significant

in the cases with dominant-side amputation. The left-side amputees who lost their nondominant hand showed comparable global FA network metrics with healthy controls. Although the power of statistical analyses might be hindered by the small sample size of the left-side amputees (n = 7), the results from the mean value suggest that alternations after nondominant-side amputation were subtle. In daily activities, people usually rely more on their dominant hand [30], and the speed, precision, and coordination of the dominant hand are superior to those of the nondominant hand [31]. Therefore, it is reasonable that loss of the dominant hand would change a lot in daily experiences and result in more extensive brain reorganization than loss of the nondominant hand.

Nodal strength analyses suggested that FA connectivity in the contralateral sensorimotor network (i.e., postcentral gyrus and paracentral lobule in the right-side amputees, and precentral gyrus in the left-side amputees) was susceptible to upper-limb amputation. We speculated that the lack of sensory input from and overt motor output to the missing limb after amputation resulted in reduced FA connectivity in the contralateral sensorimotor network. The precentral and postcentral gyri are the location of the M1 and S1, respectively, which have been demonstrated as main areas with extensive reorganization after amputation [1]. A continuous loss of GM in the contralateral M1 and S1 has been reported in a case study covering a 21-week period after upper-limb amputation [32]. Reduced GM volume in the missing hand area was also observed in upper-limb amputees compared with healthy controls [4]. Reduced interhemispheric functional connectivity of the contralateral M1 and S1 was found in animals after forelimb deafferentation [2] or upper-limb amputees [4]. Our results suggest that not only the GM and functional connectivity in the contralateral M1 and S1, but also the WM and

structural (FA) connectivity were affected by upper-limb amputation.

Reorganization in WM underlying the contralateral postcentral gyrus seems use-dependent. The nodal strength of the contralateral postcentral gyrus was reduced only in the right-side amputees, and it was negatively correlated with the residual limb usage. Our results indicated that less usage of the residual limb could help maintain the WM integrity underlying the contralateral S1 after dominant-side upper-limb amputation. This result might be associated with the compensational usage of the intact limb in daily activities and remapping of the intact limb representation into the deprived S1 cortex. After amputation, there are mainly two adaptive patterns of limb usage, i.e., relying on the intact limb [33] and using their residual limb or a prosthesis [34], and the usage of the intact limb and the residual limb are negatively correlated [4]. The left-side amputees could still rely on their dominant (intact) hand as before, and therefore they did not show significant changes in FA connectivity in the contralateral S1. While the right-side amputees usually have to use their nondominant (intact) hand extensively to compensate the loss of the dominant hand, which might result in significant reduction in FA connectivity in the contralateral S1. FMRI studies have suggested the intact limb representation might be expanded to the deprived S1 cortex, which might attribute to increased use of the intact limb [4, 35, 36]. Amputees that rely more on their intact limb (and report less frequent residual limb usage) showed increased intact limb representation in the deprived cortex [4]. In this case, the contralateral S1 cortex received sensory inputs from the intact limb after amputation, which might slow down degeneration of the WM induced by sensory deprivation from the lost limb. Intact limb fMRI activation within the deprived cortex has shown positive correlations with FA in the corticospinal tract and the inferior fronto-occipital fasciculus in the

deprived hemisphere [37]. In the present study, FA connectivity in the contralateral S1 also might be associated with the remapping of the intact limb representation into the deprived cortex, and therefore we speculate a potential positive correlation between the FA connectivity in the contralateral S1 and the intact limb usage. However, the intact limb usage was not measured. Instead, we observed a negative correlation between the residual limb usage and FA connectivity in the contralateral S1.

Both the right-side and left-side amputees showed reduced nodal strength in visual areas, such as the contralateral temporal pole/middle temporal gyrus, middle and inferior temporal gyrus, inferior occipital gyrus, the ipsilateral calcarine fissure and surrounding cortex, supramarginal gyrus, and inferior temporal gyrus in the right-side amputees, and the contralateral temporal pole/middle temporal gyrus and inferior occipital gyrus in the left-side amputees. The reduction of FA connectivity in visual areas might due to the lack of visual feedback from the missing limb. Previous studies have reported that amputees presented changes in GM or WM in the visual areas, but the results remain inconsistent. Jiang *et al.* found progressive thinning of V5/middle temporal visual area as well as a trend of cortical thinning in the V3d [38], the bilateral occipital lobes and the contralateral temporooccipital junction, and FA reduction in WM regions underlying the contralateral temporal lobe and inferior frontooccipital fasciculus [7] in lower-limb amputees. However, Preißler *et al.* found an increase in GM volume in brain regions that belong to the dorsal and ventral visual stream in upper-limb amputees [39], which also contradicts with our observation. A possible explanation for the discrepancy in upper-limb amputees might be a differential use of functional prostheses. In Preißler *et al.*'s study, more than half of the participants used a myoelectric prosthesis

regularly at an advanced level [39]; while in this study, only 4 of 21 amputees used a (cosmetic) prosthesis. It has been suggested that compensational visual feedback from prosthesis could help retain normal visual processing of hand [40]. In addition, visually control the proper action of the myoelectric prosthesis is needed in daily activities, and this enhanced need for visual control also might lead to cortical plasticity resulting in GM increase [39].

The nodal strength of the contralateral middle temporal gyrus, which was reduced in the right-side amputees, was significantly positively correlated with the PLS magnitude. The middle temporal gyrus has been suggested to be involved in sensory perception and body representation. The BOLD response in the middle temporal gyrus was significantly correlated with perceptual intensity of heat sensation [41]. Extrastriate body area (EBA), which is partially located in the middle temporal gurus, is recruited in body detection and perceiving the configuration of one's own body [42, 43]. Damage to the left temporal lobe has been found to be associated with deficits in body structural description and body image [44]. In our study, the FA connectivity of the contralateral middle temporal gyrus was reduced in amputees, which might be a result of reorganization induced by an incomplete body representation after loss of a limb. The phantom limb, which is usually perceived to be an integral part of the body by amputees [45], compensatorily substitute the missing limb so as to maintain a relatively intact body representation. Therefore, the FA connectivity of the contralateral middle temporal gyrus was less affected if amputees experienced more intensity of PLS, showing a positive correlation between the nodal strength of the contralateral middle temporal gyrus and the PLS magnitude.

In this study, the left-side and right-side amputees were analyzed respectively rather than because of the following two reasons. First, the FA network was asymmetric between two

hemispheres. The nodal strength was significantly larger in the left middle frontal gyrus, olfactory cortex, medial superior frontal gyrus, lingual gyrus, middle occipital gyrus and inferior temporal gyrus compared with the right counterparts; while the nodal strength was significantly larger in the right angular gyrus, temporal pole/ middle temporal gyrus, calcarine fissure and surrounding cortex compared with the left counterparts in healthy controls. Similarly, previous DTI studies have also reported FA asymmetry, such as a left-greater-than-right (leftward) asymmetry of the arcuate fasciculus, cingulum and corticospinal tract, and/or a rightward asymmetry of uncinate fasciculus and posterior corpus callosum [11, 24, 46]. Second, the left-side and right-side amputees showed distinct reorganization patterns from the aspect of either global metrics or nodal strength of FA network, which might be due to a differential experience induced by the loss of the dominant or nondominant hand [47]. Our results suggest that it is more reasonable to analyze the dominant- and nondominant-side amputees separately rather than to combine together and conclude from contralateral and ipsilateral aspects.

Acknowledgements

The authors thank Changzhou Disabled Persons' Federation and Jintan Disabled Persons' Federation for their help with recruitment of amputees. This work was supported by the National Basic Research Program of China (973 Program) No. 2011CB013304 and the National Natural Science Foundation of China (No. 61771313). The authors declare no conflicts of interest.

References

1. Flor, H., L. Nikolajsen, and T. Staehelin Jensen, *Phantom limb pain: a case of maladaptive CNS plasticity?* Nat Rev Neurosci, 2006. **7**(11): p. 873-81.
2. Pawela, C.P., et al., *Interhemispheric neuroplasticity following limb deafferentation detected by resting-state functional connectivity magnetic resonance imaging (fcMRI) and functional magnetic resonance imaging (fMRI).* Neuroimage, 2010. **49**(3): p. 2467-78.
3. Makin, T.R., et al., *Network-level reorganisation of functional connectivity following arm amputation.* Neuroimage, 2015. **114**: p. 217-25.
4. Makin, T.R., et al., *Phantom pain is associated with preserved structure and function in the former hand area.* Nat Commun, 2013. **4**: p. 1570.
5. Yuanyuan, L., et al., *Resting-state EEG network change in alpha and beta bands after upper limb amputation.* Conf Proc IEEE Eng Med Biol Soc, 2016. **2016**: p. 49-52.
6. Simoes, E.L., et al., *Functional expansion of sensorimotor representation and structural reorganization of callosal connections in lower limb amputees.* J Neurosci, 2012. **32**(9): p. 3211-20.
7. Jiang, G., et al., *The Plasticity of Brain Gray Matter and White Matter following Lower Limb Amputation.* Neural Plast, 2015. **2015**: p. 823185.
8. Li, Z., et al., *Altered microstructure rather than morphology in the corpus callosum after lower limb amputation.* Sci Rep, 2017. **7**: p. 44780.
9. Bullmore, E. and O. Sporns, *Complex brain networks: graph theoretical analysis of structural and functional systems.* Nat Rev Neurosci, 2009. **10**(3): p. 186-98.
10. Park, H.J. and K. Friston, *Structural and functional brain networks: from connections to cognition.* Science, 2013. **342**(6158): p. 1238411.
11. Buchel, C., et al., *White matter asymmetry in the human brain: a diffusion tensor MRI study.* Cereb Cortex, 2004. **14**(9): p. 945-51.
12. Fraser, C.M., et al., *Characterising phantom limb phenomena in upper limb amputees.* Prosthet Orthot Int, 2001. **25**(3): p. 235-42.
13. Li, X., *The distribution of left and right handedness in Chinese people.* Acta Psychol Sin, 1983. **3**: p. 268-276.
14. Flor, H., et al., *Phantom-limb pain as a perceptual correlate of cortical reorganization following arm amputation.* Nature, 1995. **375**(6531): p. 482-484.
15. Kerns, R.D., D.C. Turk, and T.E. Rudy, *The West Haven-Yale Multidimensional Pain Inventory (WHYMPI).* Pain, 1985. **23**(4): p. 345-356.
16. Cui, Z., et al., *PANDA: a pipeline toolbox for analyzing brain diffusion images.* Front Hum Neurosci, 2013. **7**: p. 42.
17. Andersson, J.L. and S. Skare, *A model-based method for retrospective correction of geometric distortions in diffusion-weighted EPI.* Neuroimage, 2002. **16**(1): p. 177-99.
18. Smith, S.M., *Fast robust automated brain extraction.* Hum Brain Mapp, 2002. **17**(3): p. 143-55.
19. Song, S.K., et al., *Dysmyelination revealed through MRI as increased radial (but unchanged axial) diffusion of water.* Neuroimage, 2002. **17**(3): p. 1429-36.
20. Tzourio-Mazoyer, N., et al., *Automated anatomical labeling of activations in SPM using a macroscopic anatomical parcellation of the MNI MRI single-subject brain.* Neuroimage, 2002. **15**(1): p. 273-89.

21. Mori, S., et al., *Three-dimensional tracking of axonal projections in the brain by magnetic resonance imaging.* Ann Neurol, 1999. **45**(2): p. 265-9.
22. Shu, N., et al., *Altered anatomical network in early blindness revealed by diffusion tensor tractography*. PLoS One, 2009. **4**(9): p. e7228.
23. Shu, N., et al., *Diffusion tensor tractography reveals disrupted topological efficiency in white matter structural networks in multiple sclerosis.* Cereb Cortex, 2011. **21**(11): p. 2565-77.
24. Takao, H., et al., *Gray and white matter asymmetries in healthy individuals aged 21-29 years: a voxel-based morphometry and diffusion tensor imaging study*. Hum Brain Mapp, 2011. **32**(10): p. 1762-73.
25. Benjamini, Y. and D. Yekutieli, *The control of the false discovery rate in multiple testing under dependency.* Annals of Statistics, 2001. **29**(4): p. 1165-88.
26. Song, S.K., et al., *Diffusion tensor imaging detects and differentiates axon and myelin degeneration in mouse optic nerve after retinal ischemia.* Neuroimage, 2003. **20**(3): p. 1714-22.
27. Harsan, L.A., et al., *Brain dysmyelination and recovery assessment by noninvasive in vivo diffusion tensor magnetic resonance imaging.* J Neurosci Res, 2006. **83**(3): p. 392-402.
28. Kraus, M.F., et al., *White matter integrity and cognition in chronic traumatic brain injury: a diffusion tensor imaging study.* Brain, 2007. **130**(Pt 10): p. 2508-19.
29. Bullmore, E. and O. Sporns, *The economy of brain network organization.* Nat Rev Neurosci, 2012. **13**(5): p. 336-49.
30. Provins, K.A., *The Specificity of Motor Skill and Manual Asymmetry: A Review of the Evidence and Its Implications.* J Mot Behav, 1997. **29**(2): p. 183-92.
31. Annett, M., *Five tests of hand skill.* Cortex, 1992. **28**(4): p. 583-600.
32. Gaser, C., et al., *Gray matter volume loss after upper limb amputation.* Klin Neurophysiol, 2004. **35**: p. 144.
33. Jones, L.E. and J.H. Davidson, *Save that arm: a study of problems in the remaining arm of unilateral upper limb amputees.* Prosthet Orthot Int, 1999. **23**(1): p. 55-8.
34. Jang, C.H., et al., *A survey on activities of daily living and occupations of upper extremity amputees.* Ann Rehabil Med, 2011. **35**(6): p. 907-21.
35. Pons, T.P., et al., *Massive cortical reorganization after sensory deafferentation in adult macaques.* Science, 1991. **252**(5014): p. 1857-60.
36. Bogdanov, S., J. Smith, and S.H. Frey, *Former hand territory activity increases after amputation during intact hand movements, but is unaffected by illusory visual feedback.* Neurorehabil Neural Repair, 2012. **26**(6): p. 604-15.
37. Makin, T.R., et al., *Deprivation-related and use-dependent plasticity go hand in hand.* Elife, 2013. **2**: p. e01273.
38. Jiang, G., et al., *Progressive Thinning of Visual Motion Area in Lower Limb Amputees.* Front Hum Neurosci, 2016. **10**: p. 79.
39. Preissler, S., et al., *Gray matter changes following limb amputation with high and low intensities of phantom limb pain.* Cereb Cortex, 2013. **23**(5): p. 1038-48.
40. Guo, X., et al., *The Effect of Prosthesis Use on Hand Mental Rotation After Unilateral Upper-Limb Amputation.* IEEE Trans Neural Syst Rehabil Eng, 2017. **25**(11): p. 2046-2053.

41. Moulton, E.A., et al., *BOLD responses in somatosensory cortices better reflect heat sensation than pain.* J Neurosci, 2012. **32**(17): p. 6024-31.
42. Downing, P.E., et al., *A cortical area selective for visual processing of the human body*. Science, 2001. **293**(5539): p. 2470-3.
43. Berlucchi, G. and S.M. Aglioti, *The body in the brain revisited.* Exp Brain Res, 2010. **200**(1): p. 25-35.
44. Schwoebel, J. and H.B. Coslett, *Evidence for multiple, distinct representations of the human body*. J Cogn Neurosci, 2005. **17**(4): p. 543-53.
45. Melzack, R., *Phantom limbs.* Sci Am, 1992. **266**(4): p. 120-6.
46. Gong, G., et al., *Asymmetry analysis of cingulum based on scale-invariant parameterization by diffusion tensor imaging.* Hum Brain Mapp, 2005. **24**(2): p. 92-8.
47. Burger, H., et al., *Validation of the orthotics and prosthetics user survey upper extremity functional status module in people with unilateral upper limb amputation.* J Rehabil Med, 2008. **40**(5): p. 393-9.